AD-A081 179 ROCKWELL INTERNATIONAL THOUSAND OAKS CA SCIENCE CENTER F/G 20/4
STUDIES OF UPPER SURFACE BLOWN AIRFOILS IN INCOMPRESSIBLE AND T--ETC(U
JAN 80 N D MALMUTH, W D MURPHY, V SHANKAR N00014-76-C-0350
UNCLASSIFIED SC5055.15TR NL

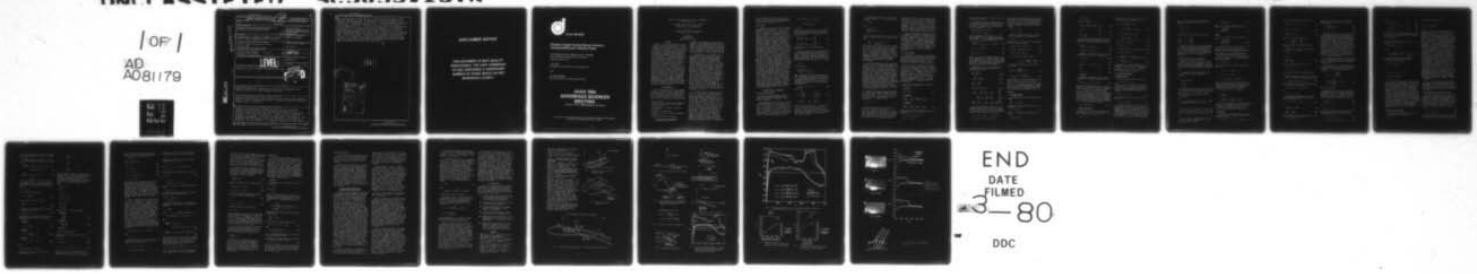

END
DATE FILMED
3-80
DDC

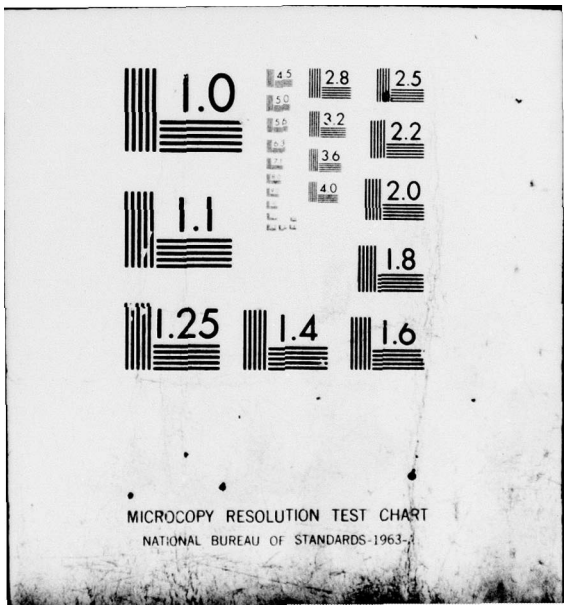
1.0
1.1
1.25
1.4
1.6
1.8
2.0
2.2
2.5
2.8
3.2
3.6
4.0
4.5
5.0
5.6
MICROCOPY RESOLUTION TEST CHART
NATIONAL BUREAU OF STANDARDS-1963-A

UNCLASSIFIED

SECURITY CLASSIFICATION OF THIS PAGE (When Data Entered)

REPORT DOCUMENTATION PAGE

READ INSTRUCTIONS BEFORE COMPLETING FORM

1. REPORT NUMBER	2. GOVT ACCESSION NO. / 3. RECIPIENT'S CATALOG NUMBER
4. TITLE (and Subtitle): STUDIES OF UPPER SURFACE BLOWN AIRFOILS IN INCOMPRESSIBLE AND TRANSONIC FLOWS	5. TYPE OF REPORT & PERIOD COVERED: Technical Report 09/30/78 through 09/30/79
	6. PERFORMING ORG. REPORT NUMBER: SC5055.15TR
7. AUTHOR(s): N.D. Malmuth, W.D. Murphy, V. Shankar, J.D. Cole (UCLA), and E. Cumberbatch (Purdue University)	8. CONTRACT OR GRANT NUMBER(s): N00014-76-C-0350
9. PERFORMING ORGANIZATION NAME AND ADDRESS: Rockwell International, Science Center, P.O. Box 1085, Thousand Oaks, California 91360	10. PROGRAM ELEMENT, PROJECT, TASK AREA & WORK UNIT NUMBERS: Task 061-234
11. CONTROLLING OFFICE NAME AND ADDRESS: Office of Naval Research, 800 North Quincy Street, Arlington, Virginia 22217	12. REPORT DATE: January 1, 1980
	13. NUMBER OF PAGES: 17
14. MONITORING AGENCY NAME & ADDRESS (if different from Controlling Office)	15. SECURITY CLASS. (of this report): UNCLASSIFIED
	15a. DECLASSIFICATION/DOWNGRADING SCHEDULE

16. DISTRIBUTION STATEMENT (of this Report)

Approved for Public Release; Distribution Unlimited

Technical rept. 30 Sep 78 - 30 Sep 79

17. DISTRIBUTION STATEMENT (of the abstract entered in Block 20, if different from Report).

18. SUPPLEMENTARY NOTES

AIAA Paper AIAA-80-0270, presented at the AIAA 18th Aerospace Sciences Meeting, January 14-16, 1980, Pasadena, California

19. KEY WORDS (Continue on reverse side if necessary and identify by block number)

Upper Surface Blowing, Jet Flaps, Propulsive Lift, Transonic Flow, Numerical Analysis, Partial Differential Equations, Programming, Asymptotic Expansions, Boundary Layers, Viscous Flow

20. ABSTRACT (Continue on reverse side if necessary and identify by block number)

Asymptotic and computational methods have been utilized to study the incompressible and transonic flow over upper surface blown airfoils. To provide a framework for more approximate simulations which are subsequently discussed, a full potential formulation is given and various numerical treatments are proposed. In this and the other models, the problem has been decomposed into the treatment of the fine structure of the jet and the analysis of the flow outside of it. Asymptotic expansions of limit process

DD FORM 1 JAN 73 1473 EDITION OF 1 NOV 65 IS OBSOLETE

389 969

UNCLASSIFIED

SECURITY CLASSIFICATION OF THIS PAGE (When Data Entered)

type have been used to treat the jet in a thin layer approximation using suitable strained variables. Although vorticity must be accounted for in matching with the external flow, its effect on the Spence boundary conditions derived under irrotational assumptions is nil in regions away from the trailing edge and jet exit. A similar conclusion applies for compressibility. The condition of flow pressure and direction compatibility replacing the Kutta condition for the unblown configuration indicates that a dividing streamline leaves tangent to the upper surface of the airfoil at the trailing edge. Computational results for a USB airfoil indicate significant enhancements in lift with blowing. Comparisons with experiments indicate that viscous wall jet effects, wave interaction phenomena with the mixing zones near the jet exit and trailing edge layers must be incorporated into the model for improved simulation of the flow physics.

DISCLAIMER NOTICE

THIS DOCUMENT IS BEST QUALITY PRACTICABLE. THE COPY FURNISHED TO DDC CONTAINED A SIGNIFICANT NUMBER OF PAGES WHICH DO NOT REPRODUCE LEGIBLY.

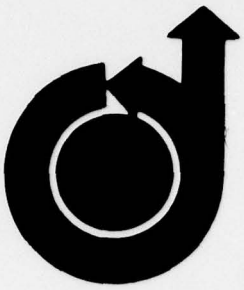

AIAA-80-0270

Studies of Upper Surface Blown Airfoils in Incompressible and Transonic Flows

N.D. Malmuth, W.D. Murphy, and V. Shankar
Rockwell International Science Center,
Thousand Oaks, CA

J.D. Cole
University of California, Los Angeles, CA

and

E. Cumberbatch
Purdue University, West Lafayette, IN

AIAA 18th AEROSPACE SCIENCES MEETING

January 14-16, 1980/Pasadena, California

STUDIES OF UPPER SURFACE BLOWN AIRFOILS IN INCOMPRESSIBLE AND TRANSONIC FLOWS[§]

N.D. Malmuth*, W.D. Murphy**, and V. Shankar**
Rockwell International Science Center
Thousand Oaks, California 91361

J.D. Cole+
University of California at Los Angeles
Los Angeles, California 90024

and

E. Cumberbatch++
Purdue University
West Lafayette, Indiana

Abstract

Asymptotic and computational methods have been utilized to study the incompressible and transonic flow over upper surface blown airfoils. To provide a framework for more approximate simulations which are subsequently discussed, a full potential formulation is given and various numerical treatments are proposed. In this and the other models, the problem has been decomposed into the treatment of the fine structure of the jet and the analysis of the flow outside of it. Asymptotic expansions of limit process type have been used to treat the jet in a thin layer approximation using suitable strained variables. Although vorticity must be accounted for in matching with the external flow, its effect on the Spence boundary conditions derived under irrotational assumptions is nil in regions away from the trailing edge and jet exit. A similar conclusion applies for compressibility. The condition of flow pressure and direction compatibility replacing the Kutta condition for the unblown configuration indicates that a dividing streamline leaves tangent to the upper surface of the airfoil at the trailing edge. Computational results for a USB airfoil indicate significant enhancements in lift with blowing. Comparisons with experiments indicate that viscous wall jet effects, wave interaction phenomena with the mixing zones near the jet exit and trailing edge layers must be incorporated into the model for improved simulation of the flow physics.

1.0 Introduction

Upper surface blowing (USB) has been proposed as a means of increasing usable lift and thereby enhancing V/STOL capability at low speeds in landing configurations. At transonic Mach numbers, it has the further application of achieving low turn radii in dogfight scenarios. The attendant high accelerations are accomplished through elimination of separation by suppression of adverse pressure gradients in the viscous boundary layer, and also movement of shocks downstream of the trailing edge, thereby discouraging shock induced separation and buffet at high maneuver incidences. Further applications of laminar flow control through stabilization using tangential blowing to achieve favorable pressure gradients is of strong interest currently.

In the application of this concept, the engine bleedoff, thrust, and structural penalties required to achieve the foregoing aerodynamic advantages is of importance to the designer. To obtain this relationship, a knowledge of the associated flow fields is required. Although attention has been given to the jet flap in theoretical investigations, relatively little analysis has been performed on upper surface blown configurations. For incompressible speeds, the work of Spence[1] represents the classical thin airfoil treatment of the jet flap problem. At transonic Mach numbers, a computational jet flap solution based on small disturbance theory was developed for airfoils, and generalized for three-dimensional wings by Malmuth and Murphy.[2-3] In these analyses, the classical Karman Guderley model was applied with a generalized version of the Murman-Cole successive line overrelaxation scheme[4] to treat the free-jet boundaries. The jet was assumed to be thin, and it was assumed on a heuristic basis that the Spence boundary conditions were applicable across it. These conditions involve equilibration between the normal pressure gradient and the centrifugal force associated with the momentum in the jet.

In this paper, the applicability of the conditions will be analyzed for a compressible rotational jet in the context of blowing upstream of the trailing edge on the upper surface, i.e., upper surface blowing in contrast to the jet flap configuration in which the jet emanates from the trailing edge. Furthermore, the thin airfoil jet flap problem formulation stipulates an initial angle of the jet at the trailing edge. In actuality, this angle is a function of the jet exit conditions and the local flow details, for jet flaps and USB. In both cases, the conditions for the trailing edge dividing streamline represent a generalization of the Kutta condition for the unblown case. The aspect of the paper involving fine-structure of the jet layer represents an extension of the earlier work of Malmuth and Murphy[5] on transonic wall jets. From these analyses, the paper will describe the numerical approach to treat the USB problem, and various results showing possibilities for lift augmentation

[§]A major portion of this effort was sponsored by the Office of Naval Research under Contract N00014-76-C-0350

*Project Manager, Fluid Dynamics, Associate Fellow AIAA

**Mathematical Sciences Group

+Professor, Structures and Mechanics Department, Fellow AIAA

++Professor, Department of Mathematics

will be presented. An additional significance of the work is its relevance to the wake curvature effects treated by Melnik and his coworkers[6] for viscous flow over transonic airfoils.

Plan of Paper

In Section 2, various formulations and analyses are provided which represent, in part, a critical assessment of different aspects of the jet flap formulation given in Ref. 1 and its extension to USB for incompressible and compressible flows. Section 2.1 gives a full potential formulation for the USB problem which can be utilized for future computational solutions and as a framework for the more approximate thin airfoil theories which are presented in subsequent sections. Candidate numerical schemes are discussed but their implementation for the full potential formulation will be reported elsewhere. As a basis for the thin airfoil and small disturbance models, the thin jet approximation is described in terms of a systematic asymptotic expansion procedure in Section 2.2 for incompressible flows. The generalization of these developments to compressible flow is straightforward and therefore not provided. Section 2.3 provides a discussion of the trailing edge region from the viewpoint of a nonuniformity of the thin jet theory as well as the generalized Kutta condition for USB. Inherent in this aspect is the geometry of the dividing streamline at the trailing edge which is a necessary condition for the determination of the jet sheet free boundary. Arguments are provided to substantiate tangency to the upper surface providing the jet stagnation pressure is greater than that of the external flow. To relate the internal jet structure to the external flow with emphasis on boundary conditions, Section 2.4 illustrates how asymptotic matching principles provide a systematic approximation to the boundary conditions for a problem for the external flow. Also indicated is how the small disturbance jet flap formulation of Ref. 1 is modified with USB. Finally, Section 3 gives results from a computational solution based on the small disturbance formulation of the earlier sections. In this section, transonic USB airfoils are analyzed and comparisons are made with experiment. Factors associated with the discrepancies are considered and refinements are proposed to improve the realism of the model.

2.0 Formulations and Analyses

2.1 Full Potential Theory

In Fig. 1, a USB configuration is shown. Before dealing with small disturbance theory, we indicate the appropriate formulation in a full potential framework.

One procedure to treat the problem is to introduce separate potentials for the internal flow in the jet region (denoted as R_j) and the external region R_e. However, it is to be noted that irrotational flow will result only if the entropy is constant across the jet exit plane AE. Thus, the model will represent a subclass of other practical cases where vorticity is introduced in the internal ducting upstream of the jet exit. Within the restrictions, the appropriate equations are

$$L[\phi_e] = \left(a^2 - \phi_{e_x}^2\right)\phi_{e_{xx}} - 2\phi_{e_x}\phi_{e_y}\phi_{e_{xy}} + \left(a^2 - \phi_{e_y}^2\right)\phi_{e_{yy}} = 0 \qquad (1a)$$

$$L[\phi_j] = 0 \qquad (1b)$$

where ϕ_e and ϕ_j are the potentials in the regions R_e and R_j, respectively. Under the assumption of irrotationality, the following energy invariants exist in R_e and R_j:

$$\frac{a_e^2}{\gamma-1} + \frac{q_e^2}{2} = \text{const.} = C_e = \frac{a_{e_0}^2}{\gamma-1} \qquad (2a)$$

$$\frac{a_j^2}{\gamma-1} + \frac{q_j^2}{2} = \text{const.} = C_j = \frac{a_{j_0}^2}{\gamma-1} \qquad (2b)$$

where the subscript 0 signifies stagnation conditions.

On the slip lines AB and CD, two sets of boundary conditions are required since these lines are free in the sense that they interact with the solution. The first of these is the tangency condition in which these lines are streamlines of the internal and external flow. Thus, on AB, which in the coordinate system indicated in Fig. 1 is given by

$$y = G_u(x)$$

the conditions are

$$\frac{\phi_{e_y}\left(x, G_u(x)\right)}{\phi_{e_x}} = \frac{\phi_{j_y}}{\phi_{j_x}} = G_u'(x) \qquad (3)$$

where the arguments of the other members are the same as the numerator of the first. In addition to (3), a jump condition obtained from Eqs. (2a) and (2b) applies across AB and ECD. This relation is synonymous with the fact the static pressure is continuous across each slip line, so that across these boundaries

$$A_e|\nabla\phi_e|^2 - A_j|\nabla\phi_j|^2 = B \qquad (4a)$$

holds, where

$$A_e \equiv \frac{p_{e_0}^{(\gamma-1)/\gamma}}{2a_{e_0}^2}, \quad A_j \equiv \frac{p_{j_0}^{(\gamma-1)/\gamma}}{2a_{j_0}^2} \qquad (4b)$$

$$B \equiv \left[p_{e_0}^{(\gamma-1)/\gamma} - p_{j_0}^{(\gamma-1)/\gamma}\right] \Big/ 2(\gamma-1) . \qquad (4c)$$

Similar conditions hold on ECD. In addition to (3) and (4), suitable conditions on the slope of AB and ECD at the trailing edge A and C are required to complete this part of the formulation. These would be determined by continuity of pressure and flow angle at these locations, presumably by some iterative procedure.

On the surface of the airfoil, a condition of the type (3) applies, i.e., if the upper surface is given by

$$y = F_u(x)$$

then

$$\frac{\phi_{e_y}\left(x,F_u(x)\right)}{\phi_{e_x}\left(x,F_u(x)\right)} = F_u'(x) \ .$$

A similar relation holds for the lower airfoil surface. For the far field, in R_e, a relation of the type

$$\phi = \frac{\Gamma\theta}{2\pi} \quad , \quad \text{as } r^2 = x^2 + Y^2 \to \infty$$
$$(Y = \text{scaled } y)$$

apolies approximately, where Γ is the circulation on a circuit at $r = \infty$ and $\theta = \tan^{-1} Y/x$. Note that the circuit includes contributions along the jet. The far field in R_i can be obtained by methods similar to that developed by Malmuth and Murphy in Ref. 5. To complete the formulation, initial conditions at the jet exit and a suitable far field downstream are required. If the former is subsonic, Neumann or Dirichlet data are appropriate. If it is supersonic, then Cauchy data are necessary. Downstream, data are used only if the flow is locally subsonic.

At least three alternatives appear possible for the solution of the aforementioned boundary value problem. In the first, no mappings are applied and the problems are to be solved in the physical (Cartesian) plane. This approach has the advantage of allowing highly developed techniques to be applied to the Cartesian form of the full potential equations (FPE). Successful implementation would, however, require means of dealing with the movable free boundaries. In particular, stable extrapolative and interpolative procedures would have to be developed to handle large free boundary shifts between grid points, with minimum error propagation. In the Cartesian equation approach, it is envisioned that the problem would be solved separately in domains in R_i and R_e on alternate cycles using successive line overrelaxation (SLOR). Conditions in the other domain would be updated using "latest" data from either Eq. (3) or (4).

The second method would use mapping procedures such as those due to Thompson. Another possibility is to open up the cut physical plane with the mapping $w = \sqrt{z}$, where $z = x + iy$ and $w = u + iv$. In this mapping, the jet boundaries would project as lines $v = S(u)$. A subsequent shearing transformation

$$v' = v - S(u)$$

$$u' = u$$

would bring the free boundary on the real axis. Yet another mapping procedure would be $(x,y) \to (x,\psi)$, where ψ is the stream function satisfying the exact continuity equations. The advantage of these mappings is that they would "freeze" the free boundaries. A disadvantage is that they would compromise the equation in the sense that a new numerical method would probably have to be developed to effectively capture shocks and treat the mixed field in an accurate and computationally efficient way. Issues of stability, diagonal dominance would have to be resolved. Similar questions would also arise in connection with a third formulation involving the stream function ψ as a dependent variable. In contrast to the independent variable case where the free boundary position is known with unknown boundary conditions, this would generate an unknown boundary carrying known data.

In spite of the attendant problem areas in the full potential formulation, it represents a desirable longer range objective to treat thick configurations and assess the accuracy of small disturbance USB solutions. In the short term, the small disturbance solution has been implemented because of its simplicity of extension to three dimensions and its ease in integration with other inverse procedures that we have developed to remove shocks on unblown airfoils. Within this framework, the free boundaries can be more easily treated due to the appropriateness of transfer of boundary conditions.

2.2 Thin Jet Theory

As an essential ingredient of a small disturbance formulation, the jet structure is developed in this section for purposes of specification of the boundary conditions. In particular, it will be shown how the Spence theory of Ref. 1 can be derived from a systematic approximation procedure.

Referring to Fig. 2, a section of the jet is shown. A curvilinear coordinate system is embedded in the jet as indicated. The lines η = constant are parallel to a reference line (the ξ axis) which only under special circumstances coincides with the centerline of the jet. Otherwise, the ξ axis is a reference line which is the centerline of an approximate parallel flow to be discussed subsequently. In this coordinate system, the lines ξ = constant are normals to ξ axis. In what follows, the incompressible case will be discussed. The generalizations to compressible flow are straightforward.

Within the indicated coordinate system, the exact equations of motion are

Continuity

$$\frac{\partial}{\partial\xi} q_\xi + \frac{\partial}{\partial\eta} h\, q_\eta = 0 \qquad (5a)$$

ξ - Momentum

$$\frac{q_\xi}{h}\frac{\partial q_\xi}{\partial\xi} + q_\eta \frac{\partial q_\xi}{\partial\eta} + \frac{q_\xi q_\eta}{h}\frac{\partial h}{\partial\eta} = \frac{-1}{\rho}\frac{\partial p}{\partial\xi} \qquad (5b)$$

η - Momentum

$$\frac{q_\xi}{h}\frac{\partial q_\eta}{\partial\xi} + q_\eta \frac{\partial q_\eta}{\partial\eta} - \frac{q_\xi^2}{h}\frac{\partial h}{\partial\eta} = -\frac{1}{\rho}\frac{\partial p}{\partial\eta} \qquad (5c)$$

where h, the metric coefficient when related to the differential arc length in Cartesian (x,y) coordinates is

$$dx^2 + dy^2 = h^2(\xi,\eta)d\xi^2 + d\eta^2$$

$$h(\xi,\eta) = 1 - \eta/R(\xi) \qquad (6)$$

with $R(\xi)$ being the radius of curvature which is shown positive in Fig. 2.

To obtain an approximate incompressible set of equations prototypic of the compressible case, the thin jet limit is considered. The characteristic jet thickness is shown in Fig. 2, where the jet boundary is denoted as $\eta = \tau b(\xi)$.

We now define a thin jet limit

$$\tau \to 0,\ \xi, \eta^* = \eta/\tau \text{ fixed} \tag{7}$$

where the boundary layer coordinate η^* is introduced to keep the jet slip lines in view in the limit process. In (7), the appropriate representations to yield a nontrivial structure are

$$\frac{q_\xi(\xi,\eta;\tau)}{U} = \frac{1}{\sqrt{\tau}} u_0(\xi,\eta^*) + \sqrt{\tau}\, u_1(\xi,\eta^*) + \cdots \tag{8a}$$

$$\frac{q_\eta}{U} = \sqrt{\tau}\, v_0 + \tau^{3/2} v_1 + \cdots \tag{8b}$$

$$\frac{p}{\rho U^2} = p_0 + \tau p_1 + \cdots \tag{8c}$$

where U is some typical freestream velocity. The orders were selected to give the "richest" possible set of equations and, consistent with this, produce forcing terms in the equations for the second order quantities. These orders are consistent with the massless momentum source model of Spence.[1]

Substitution of (8) in (5) and equating like orders gives the following equations for the approximate quantities:

$$\left.\begin{aligned} &\frac{\partial u_0}{\partial \xi} + \frac{\partial v_0}{\partial \eta^*} = 0 \qquad (9a)\\ &u_0 \frac{\partial u_0}{\partial \xi} + v_0 \frac{\partial u_0}{\partial \eta^*} = 0 \qquad (9b)\\ &\frac{u_0^2}{R(\xi)} = -\frac{\partial p_0}{\partial \eta^*} \qquad (9c) \end{aligned}\right\}$$

$$\left.\begin{aligned} &\frac{\partial u_1}{\partial \xi} + \frac{\partial v_1}{\partial \eta^*} = \frac{1}{R}\frac{\partial}{\partial \eta^*}(\eta^* v_0) \qquad (10a)\\ &u_0 \frac{\partial u_1}{\partial \xi} + v_0 \frac{\partial u_1}{\partial \eta^*} + \frac{\partial u_0}{\partial \xi} u_1 + \frac{\partial u_0}{\partial \eta^*} v_1 \\ &\quad = \frac{u_0 v_0}{R} - \frac{\eta^*}{R} u_0 \frac{\partial u_0}{\partial \xi} - \frac{\partial p_0}{\partial \xi} \qquad (10b)\\ &\frac{2u_0 u_1}{R} + \frac{\partial p_1}{\partial \eta^*} = -u_0 \frac{\partial v_0}{\partial \xi} - v_0 \frac{\partial v_0}{\partial \eta^*} - \frac{u_0^2 \eta^*}{R^2} \qquad (10c) \end{aligned}\right\}$$

The appropriate boundary conditions involve statements regarding the fact that the jet boundaries are streamlines and that the static pressure is continuous across the slip lines. The upper and lower slip lines S_u and $S_\ell = 0$ are given by

$$S_u = \eta - \tau b_0(\xi) - \tau^2 b_1(\xi) = 0 \ , \ (b_1(\xi_{TE}^+) = 0)$$

$$S_\ell = \eta + \tau b_0(\xi) + \tau^2 b_1(\xi) H(\xi - \xi_{TE}) = 0$$

where symmetry has been assumed to leading order, and the jet flow has been divided into two portions $\xi < \xi_{TE}$ and $\xi > \xi_{TE}$, with ξ_{TE} representing the trailing edge position and the fact that the trailing edge is a streamline (no jet width perturbation) is introduced by the Heaviside function H, defined as

$$H(x) = 0 \ , \ x \leq 0$$

$$= 1 \ , \ x > 0 \ .$$

Based on the foregoing discussion, the condition that jet boundaries S are streamlines is

$$\vec{q} \cdot \nabla S = 0$$

where $\vec{q} = (q_\xi, q_\eta)$. Substitution of the expansions (8) into this relation gives:

$$\left.\begin{aligned} &v_0(\xi, b_0) = b_0'(\xi)\, u_0(\xi, b_0) \qquad (11a)\\ &v_0(\xi, -b_0) = -b_0'(\xi)\, u_0(\xi, -b_0) \qquad (11b) \end{aligned}\right\}$$

$$v_1(\xi, b_0) = b_1'(\xi)\, u_0(\xi, b_0) \qquad (11c)$$

$$v_1(\xi, -b_0) = -b_1'(\xi)\, u_0(\xi, b_0) + b_0' b_0 + b_0' \left(u_1 + b_1 \frac{\partial u_0}{\partial \eta^*}\right) - b_1 \frac{\partial v_0}{\partial \eta^*} \ . \qquad (11d)$$

The other conditions involving continuity of pressure are:

$$p_0(\xi, b_0) = \frac{p_{ext}^{(u)}(\xi)}{\rho U^2} \equiv q_u(\xi) \tag{12a}$$

$$p_1(\xi, b_0) = -\, b_1(\xi) \frac{\partial p_0}{\partial \eta^*}(\xi, b_0) \tag{12b}$$

where we assume for the present argument that the external pressure field $p_{ext}^{(u)}$ is prescribed. In addition, $\tau \ll \delta$ has been also implicitly assumed. For $\tau = O(\delta)$, (12b) would be presumably changed to reflect a second order perturbation of the outer flow. In actuality, it is determined iteratively and interacts with the internal jet flow.

Solutions

First Order Theory

We introduce the zeroth order stream function given by

$$\frac{\partial \psi}{\partial \xi} = -\, v_0 \ , \ \frac{\partial \psi}{\partial \eta^*} = u_0$$

and employ the following transformation for the independent variables

$$(\xi, \eta^*) \to (\xi, \psi) \ . \tag{13}$$

Under (13), the differential operators map as follows:

$$\frac{\partial}{\partial \xi} = \frac{\partial}{\partial \xi} - v_0 \frac{\partial}{\partial \psi}$$

$$\frac{\partial}{\partial n^*} = u_0 \frac{\partial}{\partial \psi}$$

and Eqs. (9) become

$$\left.\begin{aligned} &\frac{\partial u_0}{\partial \xi} - v_0 \frac{\partial u_0}{\partial \psi} + u_0 \frac{\partial v_0}{\partial \psi} = 0 && (14a)\\ &\frac{\partial u_0}{\partial \xi} = 0 && (14b)\\ &\frac{u_0}{R} = -\frac{\partial p}{\partial \psi} . && (14c) \end{aligned}\right\}$$

For simplicity and without excessive loss of generality, we consider a constant velocity jet exit (ξ=0) initial profile parallel to the wall, i.e.,

$$\frac{q_\xi(0,n^*)}{U} = C \Rightarrow u_0(0,n^*) = C \qquad (15a)$$

$$q_n(0,n^*) = 0 = v_0(0,n^*) . \qquad (15b)$$

Equations (14) have the following solutions on application of (15), (11a), (11b) and (12a):

$$\left.\begin{aligned} &u_0 = u_0(\psi) = C && (16a)\\ &v_0 = 0 && (16b)\\ &p_0(\xi,n^*) = (1-n^*)\frac{C^2}{R} + q_u(\xi) && (16c)\\ &b_0 = 1 && (16d)\\ &\psi = Cn^* . && (16e) \end{aligned}\right\}$$

Discussion

Equations (16) describe a parallel flow jet. The total jump in pressure across the jet from (16c) is

$$[p_0] = p(\xi,1) - p(\xi,-1) = 2C^2/R \qquad (17)$$

which agrees with the Spence model. It should be noted that in contrast to the latter, no assumption regarding irrotationality is required to obtain (17), in contrast to the results of previous workers. The radius of curvature of the jet is approximately R upstream of the trailing edge which in turn is approximately given by that of the blown upper surface. Downstream of the trailing edge, R is determined from applying (17) to the determination of the flow outside of the jet. Upstream of the trailing edge, the wall pressure is determined by (17) since R is known and is given by

$$p(\xi,-1) = \frac{2C^2}{R} + q_u(\xi) . \qquad (18)$$

Second Order Theory

Equations (10) have been solved subject to the boundary conditions (11c), (11d), (12b) and the initial condition at the jet exit ξ=0

$$u_1(0,n^*) = 0$$

to give the following solution, where the first order solution (16) is assumed:

$$\left\{\begin{aligned} &v_1 = v_1^{(R)} = \frac{q_u'(\xi)}{u_0} n^* + u_0(1/R)' \\ &\qquad \times \left[n^* + \frac{1-n^{*2}}{2}\right] , \ 0 \le \xi < \xi_{TE} && (19a)\\ &v_1 = v_1^{(L)} = \frac{q_u'}{u_0}[1+n^*] + u_0(1/R)' \\ &\qquad \times \left[\frac{3}{2} + n^* - \frac{n^{*2}}{2}\right] , \ \xi > \xi_{TE} && (19b)\\ &v_1(\xi_{TE}^+,-1) = -q_\ell'(0+)/u_0 && (19c)\\ &v_1(\xi_{TE}^-,-1) = 0 && (19d)\\ &u_1 = u_0(1-n^*)[R(0)^{-1} - R^{-1}] + (q_u(0) - q_u)/u_0 && (19e)\\ &b_1 = 2[q_u - q_u(0)]/u_0^2 && (19f)\\ &p_1 = \frac{2u_0^2}{RR(0)}\left[\frac{n^{*2}}{2} - n^* + \frac{1}{2}\right] + \frac{u_0^2}{R^2}\left[2n^* - \frac{3}{2}n^* - \frac{1}{2}\right] \\ &\qquad - \frac{2n^*}{R}[q_u(0) - q_u] . && (19g) \end{aligned}\right.$$

Besides $u_0 \to 0$, another nonuniformity is evident in (19a) and (19c) and is associated with the factor $q_u'(\xi)$ as $\xi \to \xi_{TE}$, if the latter approaches ∞. As we will see, this occurs for trailing edge angles less than 60°.

2.3 Trailing Edge Behavior

Incompressible Flows

Defining the complex potential function as

$$F(z) = \phi(x,y) + i\psi(x,y)$$

where (x,y) is the local coordinate system shown in Fig. 3 and z = x+iy, the local "corner flow" solution to within a dimensional multiplicative constant in the lower external region A'OB with β as the dividing streamline angle shown is given by

$$F = e^{-i\pi(\pi-\nu)/\beta} z^{\pi/\beta} \qquad (20)$$

which implies that the square of the resultant velocity q is

$$|F'|^2 = q^2 \sim r^{2\left(\frac{\pi}{\beta} - 1\right)} . \qquad (20')$$

To obtain the necessary initial conditions for determination of the jet, the implications of continuous pressure and flow angle across the dividing streamline near the trailing edge were studied for incompressible flow. Referring to Fig. 3, with the dividing streamline denoted as OB, we signify the trailing edge angle as ν, the angle that OB makes with the upper surface AO as ω and that with the lower surface as β. In what follows, we identify

each of nine possible cases that can occur with the following shorthand notation exemplified as follows:

$$LG \Rightarrow \omega < \pi,\ \beta > \pi$$

$$EG \Rightarrow \omega = \pi,\ \beta > \pi$$

$$(\beta = 2\pi - \omega - \nu) .$$

The "truth table" indicating the nine cases is

$$\begin{pmatrix} LL & LG & LE \\ GL & GG & GE \\ EL & EG & EE \end{pmatrix} .$$

Introducing the notation in which + subscripts and superscripts signify conditions above AB and - subscripts and superscripts denote points below this line, we now examine each of the possibilities. In what follows, let p_0 be the stagnation pressure and p be its static value. Except where otherwise noted, we will also assume that $p_0^{(+)} > p_0^{(-)}$.

All Possibilities Involving G Except GG

These must be ruled out on the basis that on the G side, $p = -\infty$ which is unphysical on its own merits. Furthermore, p would equal p_0, the stagnation value on the L side, and equality of pressure across the slip line would therefore be impossible.

GG

This must be excluded since it would imply $\beta + \omega > 2\pi$ which is clearly geometrically impossible.

LL

This implies that

$$p^+ = p_0^+$$

$$p^- = p_0^- .$$

To realize pressure equality across the slip lines, this must be ruled out as impossible for all cases except when $p_0^+ = p_0^-$. This also is a corollary of the Kutta condition applicable to unblown configurations.

EE

This is associated with $\nu = 0$, i.e., a cusped trailing edge or flat plate for $p_0^+ = p_0^-$.

LE

Here, $p^- < p_0^- < p_0^+$. However, $p^+ = p_0^+$ in this case which makes equilibration of the static pressures p^- and p^+ impossible across the slip line AB.

EL

This is the only viable possibility. Here, $p^+ < p_0^+$. In fact, by Bernoulli and slip line pressure continuity, we have

$$p^+ = p_0^+ - \frac{\rho u^{+2}}{2} = p^- = p_0^- \qquad (21)$$

where u^+ is the upper stream speed at 0. To satisfy (21), the "slip" velocity u^+ is thus

$$u^+ = \sqrt{\frac{2(p_0^+ - p_0^-)}{\rho}} \qquad (22a)$$

Remarks

If $p_0^+ < p_0^-$, then LE is the only possibility with

$$u^- = \sqrt{\frac{2(p_0^- - p_0^+)}{\rho}} . \qquad (22b)$$

For a hypothetical case in which $p_0^- \approx p_0^+$ in a real physical flow (fluctuating above and below equality), then a tri-stable configuration could evolve which would oscillate between LL, LE and EL.

Nonuniformities of Second Order Approximation

From (20), we find that the other nonuniformity referred to following Eq. (19) is associated with the following behavior

$$q_u' \sim r^{(2\pi/\beta)-3} \quad \text{as} \quad r \to 0$$

where, we distinguish the following possibilities as $\xi \to \xi_{TE}$:

(i) $q_u' \to \infty$, $\beta > \frac{2\pi}{3}$ or $\nu < \frac{\pi}{3}$

(ii) $q_u' \to 0$, $\beta < \frac{2\pi}{3}$ or $\nu > \frac{\pi}{3}$

(iii) q_u' finite $\neq 0$, $\beta = \frac{2\pi}{3}$ or $\nu = \frac{\pi}{3}$.

Case (i) is the most practical situation and will necessitate an inner solution for the transition layer to join the wall and free jet flows. Before considering this, we briefly investigate the vorticity which can be shown to be given by $\omega = \tau^{-3/2}\,\omega_0 + \tau^{-1/2}\,\omega_1 + \cdots$, where

$$\omega_0 = \frac{\partial u_0}{\partial n^*} = 0$$

$$\omega_1 = \frac{\partial u_1}{\partial n^*} - \frac{u_0}{R} = -\frac{C}{R(0)} = \text{constant} \neq 0 .$$

In spite of the constant initial flow, a non-zero vorticity is thus introduced by the body curvature. By contrast, a potential vortex over a circular cylindrical surface would have had a linear initial profile to produce an irrotational flow.

Inner Problem

Anticipating large gradients near $\xi = \xi_{TE}$ we consider the following asymptotic expansions valid in the inner limit

$$\xi^* = (\xi - \xi_{TE})/\lambda(\tau) , \quad n^* = n/\tau \text{ fixed as } \tau \to 0 \qquad (23)$$

where C has been assumed to be unity in (16):

$$\frac{q_\xi}{U} = \frac{1}{\sqrt{\tau}} + \alpha(\tau)u^*(\xi^*,\eta^*) + \cdots \tag{24a}$$

$$\frac{q_\eta}{U} = \beta(\tau)v^*(\xi^*,\eta^*) + \cdots \tag{24b}$$

$$\frac{p-\bar{p}}{\rho U^2} = p^*(\xi^*,\eta^*) + \cdots \tag{24c}$$

where, $\bar{p}$ is a reference pressure and

$$h = 1 - \frac{\eta}{R^*(\xi^*)} = 1 - \frac{\tau\eta^*}{R^*} .$$

Here, R* represents the centerline radius of curvature.

To obtain the richest continuity equation assuming $R^* > O(\tau)$, we put

$$\frac{\alpha}{\lambda} = \frac{\beta}{\tau}$$

to give

$$\frac{\partial u^*}{\partial \xi^*} + \frac{\partial v^*}{\partial \eta^*} = 0 . \tag{25}$$

Roughly, the matching condition for u* is

$$\left.\begin{array}{l}\xi^* \to -\infty \\ \xi \to 0\end{array}\right\} \quad u^* \to 0 .$$

For v*, we introduce the intermediate variable $\xi_\nu = \xi/\nu(\tau)$.

Matching the inner and outer solutions by writing each in intermediate variables, we assert that

$$\beta(\tau)v^*\left(\frac{\nu}{\lambda}\xi_\nu,\eta^*\right) \Rightarrow \sqrt{\tau}\, b_0'(\nu\xi_\nu)u_0(\psi) \tag{26}$$

where the double arrow signifies asymptotic equality. Equation (26) implies that

$$b_0'(0) = v^*(-\infty,\eta^*) = \text{constant} = 0$$

and

$$\beta = \sqrt{\tau} , \quad \alpha/\lambda = 1/\sqrt{\tau} .$$

Substituting the expansions (24) into the momentum equations, the remaining equations in the distinguished limit

$$\lambda = \tau , \quad \beta = \sqrt{\tau} , \quad \alpha = \sqrt{\tau} \tag{27}$$

are

$$\frac{\partial v^*}{\partial \xi^*} + \frac{1}{R^*} = -\frac{1}{\rho}\frac{\partial p^*}{\partial \eta^*} \tag{28a}$$

$$\frac{\partial u^*}{\partial \xi^*} = -\frac{1}{\rho}\frac{\partial p^*}{\partial \xi^*} . \tag{28b}$$

Equation (28b) can be integrated directly to give the linearized Bernoulli relation

$$u^* = -\frac{p^*}{\rho} + F(\eta^*)$$

where F is an arbitrary function of integration. The system (28) is equivalent to the following scalar equations

$$\Delta p^* = \frac{\partial^2 p^*}{\partial \xi^{*2}} + \frac{\partial^2 p^*}{\partial \eta^{*2}} = 0 \tag{29a}$$

$$\Delta v^* = (-1/R^*)' . \tag{29b}$$

The appropriate boundary value problem for (29) involves specializations of boundary conditions already discussed and conditions obtained from matching at the upstream and downstream boundaries of a rectangular domain. The jet boundaries are not free to this order, being at $\eta^* = \pm 1$. A complete solution of the problem subject to these conditions is in progress. As an interim step, a special form of an "inner inner" solution is indicated for the jet flow immediately above the trailing edge. To illustrate the singular behavior, vorticity associated with a source term in the Poisson equation for u obtained from (28) and (25) is suppressed by a choice of suitable jet exit conditions. In addition, the right hand side of (29b) is assumed to vanish by linearization about $\xi = \xi_{TE}$ in the subscale assumed.

For purposes of the analysis, the configuration in Fig. 3 is considered. Here, $\omega = \pi$, representing the EL arrangement which was proven previously to be appropriate.

On applying Bernoulli's theorem on the upper and lower sides of the trailing edge, and employing the condition that the pressure is continuous across the dividing streamline OB we obtain using (20')

$$u^+ \equiv u(x,0+) = \sqrt{\frac{p_0^+ - p_0^-}{\rho}} \times \left[1 + \frac{\pi^2}{2\beta^2}\frac{x^{2\left(\frac{\pi}{\beta}-1\right)}}{\frac{p_0^+ - p_0^-}{\rho}} + \cdots\right] \quad \text{as } x \to 0 \tag{30}$$

where ρ is the density.

The solution for the jet flow in the immediate neighborhood of the trailing edge satisfies the appropriate boundary value problem for the upper half plane $y > 0$ (Fig. 4) in which flow angle and pressure are matched. Here, continuity of flow turning signifies that in some "inner" region

$$v(x,0) = 0 , \quad x < 0 \tag{31a}$$

$$v(x,0) \to 0 , \quad x \to 0 \tag{31b}$$

and

$$u(x,0+) = A + Bx^\alpha \tag{32}$$

where A and B are constants determined from (31). The appropriate harmonic functions satisfying (31) and (32) are

$$F'(z) = a_0 + a_1 e^{-i\pi\alpha} z^\alpha \tag{33a}$$

$$u = a_0 + a_1 r^\alpha \cos \alpha(\theta-\pi) = \text{Re } F'(z) \tag{33b}$$

for which

$$u(x,0) = a_0 + a_1 x^{\alpha} + \cdots \quad , x \to 0 \qquad (34a)$$

$$u(x,0) = a_0 + a_1 x^{\alpha} \cos \alpha\pi + \cdots \quad , x \to 0 \qquad (34b)$$

$$v(x,0) = 0 \quad , x \to 0 \qquad (34c)$$

$$v(x,0) = -a_1 x^{\alpha} \sin \alpha\pi \quad , x \to 0 \ . \qquad (34d)$$

The shape of the slip line is determined by applying Eqs. (34) in the tangency relation. Denoting the jet boundary by

$$J = y - B(x) = 0$$

then the flow tangency relation $(u,v) \cdot \nabla B = 0$ implies that

$$B'(x) = \arg F' \Big|_{y=B(x)}$$

so that

$$B' = \frac{a_1 x^{\alpha}}{a_0 + a_1 x^{\alpha} \cos \alpha\pi} = \frac{a_1}{a_0} x^{\alpha} + \cdots \text{ as } x \to 0 \qquad (35)$$
$$\text{for } \beta < \pi \ .$$

Hook of Dividing Streamline — Discussion

Equation (35) implies that

$$B''(x) = -\alpha \frac{a_1}{a_0} x^{\alpha-1} \ .$$

Thus

$$B''(x) \to \infty \text{ as } x \to 0 \text{ if } \nu < \frac{\pi}{3}$$

in spite of the fact that

$$B'(x) \to 0 \text{ as } x \to 0 \ ,$$

i.e., a "hook" of infinite curvature but with zero slope develops at the intersection of the dividing streamline and the trailing edge. This fact has significant consequences regarding the generation of lift of blown airfoils. In this context, the classical Spence solution fails to treat this detail since it is cast in a thin airfoil theory framework. It gives a logarithmic singularity at the trailing edge in contrast to that of the solution above. The representation of B near x=0 from (35) provides the initial conditions for the determination of the lower boundary of the jet and the vorticity it carries. This in turn determines the running circulation and the total lift. A systematic matching procedure to join this solution to the outer flow and achieve a consistent numerical formulation has apparently not been reported in the literature, even for the unblown incompressible case corresponding to thin airfoil theory, i.e., for $\nu \ll 1$.

Compressible Trailing Edges

Consider again the configuration of Fig. 3. Here we analyze first the case where

$$p_0^+ > p_0^- \ .$$

With the usual isentropic relation

$$\frac{p^+}{p_0^+} = \left[1 + \frac{\gamma-1}{2} M^2\right]^{\frac{-\gamma}{\gamma-1}} \ ,$$

the local Mach number, M, can adjust in a continuous way in order that the flow recompresses smoothly from B to 0. At 0, M is single valued=M_1 and adjusts itself such that the pressure p^+ equals p_0^-, in accord with the isentropic relation, assuming that the flow stagnates at 0 on the lower side. The only way this can be realized is with an EL configuration. By contrast, a discontinuous transition can occur and is illustrated schematically in Fig. 5a, and is associated with a GL arrangement. In some respects the configuration resembles flow over a solid wall expansion corner consisting of expansion fan interacting with a sonic line from the corner. If the solid configuration were representative of this flow with the free boundary slip line, compression waves would reflect off the sonic line and form a shock envelope which would be necessary to recompress the flow from an overexpanded value below the critical p_*^+ to the p_0^- level. Additional reflections can be produced from the upper slip line CD. This discontinuous transition leads to a multivalued pressure at 0. The continuous and discontinuous processes are illustrated schematically in Figs. 5b and 5c, respectively. In Fig. 5b, the recompression takes place on the line 80. In Fig. 5c it occurs on 00'0"0"' signifying the confluence of multiple states at 0. Here, the dashed line element 0"0"' signifies a shock jump. Experimental data strongly suggests that as in the incompressible case, the EL configuration is the most probable situation, since on a qualitative basis, it represents a path of least resistance. Presumably, a more rigorous argument to support this conjecture would rely on some sort of stability analysis.

For $p_0^+ = p_0^-$, the dividing streamline would again bisect the trailing edge since the flow in the immediate vicinity would be incompressible and the reasoning in the previous section would apply. For the improbable case of $p_0^+ < p_0^-$ the LE configuration would be applicable as for the incompressible situation.

2.4 Incompressible Small Deflection Theory

Because of its potential value for simplified treatment of the trailing edge neighborhood and matching with the outer flow, we consider in this section a small deflection specialization of the previous thin jet theory. For purposes of illustrating the theory, we revert back to incompressible flow. We consider a section of the jet far away from the trailing edge region depicted in Fig. 6. The upper and lower slip lines are given by

$$J_u = y - \delta b_u(x) = 0 \qquad (36a)$$

$$J_\ell = y - \delta b_\ell(x) = 0 \qquad (36b)$$

where the slope of the slip line is assumed to be of the same order of the characteristic thickness

ratio δ or incidence α of the airfoil. Moreover, (36) implies that the jet thickness is also of the same order.

We assume asymptotic expansions for the velocity vector $\vec{q}$ and pressure P can be written in the form

$$\frac{\vec{q}(x,y;\delta)}{U} = \left[\alpha_0(\delta)u_0(\tilde{x},\tilde{y}) + \alpha_1 u_1 + \cdots\right]\vec{i} + \left[\beta_0(\delta)v_0 + \cdots\right]\vec{j} + \cdots \tag{37a}$$

$$\frac{P - P_\infty}{\rho U^2} = \kappa_0(\delta)p_0 + \kappa_1(\delta)p_1 + \cdots \tag{37b}$$

for $x = \tilde{x}, \tilde{y} = \dfrac{y - \delta b_\ell(x)}{\delta}$ fixed as $\delta \to 0$, where U is the freestream velocity, ρ is the density, and P_∞ is the ambient pressure. The condition that the lower slip line is a streamline of the jet flow reads

$$\vec{q} \cdot \nabla J_\ell = 0$$

which to dominant order implies

$$v_0(x,0) = \frac{\delta\alpha_0}{\beta_0} b_\ell'(x) \tag{38a}$$

which provides a non-trivial case only if

$$\frac{\delta\alpha_0}{\beta_0} = 1 \ . \tag{38b}$$

Based on (38b), a similar relation is obtained on the upper slip line which is

$$v_0(x, b_u - b_\ell) = b_u'(x) \ . \tag{38c}$$

On substitution of (37) and (38b) into the exact incompressible Euler equations, the following system evolves:

x Momentum

$$Du_0 = -\frac{\kappa_0}{\alpha_0^2} p_{0_x} \tag{39a}$$

y Momentum

$$Dv_0 = -\frac{\kappa_0}{\delta^2\alpha_0^2} p_{0_{\tilde{y}}} \tag{39b}$$

Continuity

$$u_{0_x} + v_{0_{\tilde{y}}} = 0 \tag{39c}$$

where

$$\frac{\partial}{\partial x} = \frac{\partial}{\partial \tilde{x}} - b_\ell' \frac{\partial}{\partial \tilde{y}} \ , \quad D = u_0 \frac{\partial}{\partial x} + v_0 \frac{\partial}{\partial \tilde{y}} \ .$$

On inspection of the system (39), we note the following possibilities

$$\text{(i)} \quad \frac{\kappa_0}{\delta^2\alpha_0^2} \to 0$$

$$\text{(ii)} \quad \frac{\kappa_0}{\delta^2\alpha_0^2} = 1$$

$$\text{(iii)} \quad \frac{\kappa_0}{\delta^2\alpha_0^2} \to \infty \ . \tag{40}$$

Case (ii) appears to be the most interesting of the three since (i) leads to constant vertical and horizontal velocity along streamlines which restricts the free surface shape and (iii) leads to no pressure difference across the jet to this order which is of limited practical interest. For case (ii), we introduce the stream function mapping

$$(x,\tilde{y}) \to (\hat{x},\psi) \tag{41}$$

in which

$$\hat{x} = \tilde{x} = x$$

$$u_0 = \psi_{\tilde{y}} \ , \quad v_0 = -\psi_x$$

$$\frac{\partial}{\partial x} = \frac{\partial}{\partial \hat{x}} - v_0 \frac{\partial}{\partial \psi}$$

$$\frac{\partial}{\partial \tilde{y}} = u_0 \frac{\partial}{\partial \psi}$$

$$D \equiv u_0 \frac{\partial}{\partial \hat{x}} \ .$$

Under (40) with (41), Eqs. (39) become

x Momentum

$$u_0 \frac{\partial u_0}{\partial \hat{x}} = 0 \tag{42a}$$

y Momentum

$$\frac{\partial v_0}{\partial \hat{x}} = \frac{\partial p_0}{\partial \psi} \tag{42b}$$

Continuity

$$\left(\frac{\partial}{\partial \hat{x}} - v_0 \frac{\partial}{\partial \psi}\right) u_0 + u_0 \frac{\partial v}{\partial \psi} = 0 \ . \tag{42c}$$

The solution of (42) subject to the boundary conditions is

$$u_0 = U(\psi) \tag{43a}$$

$$v_0 = b_\ell'(x)U(\psi) \tag{43b}$$

$$p_u - p(x) = -b_\ell'(x) \int_\psi^{\psi_u} U(\psi')d\psi' \ . \tag{43c}$$

Here, $p_\ell(x)$ and $b_\ell(x)$ are the pressure and slope of the lower slip line of the jet. Eqs. (43) indicate that the horizontal velocity component is

convected along streamlines from a prescribed initial distribution at some upstream station. If this distribution is constant, i.e., if

$$u_0(0,\psi) = C ,$$

then (43) specializes to

$$u_0 = C \tag{44a}$$

$$v_0 = C\, b_u'(x) \tag{44b}$$

$$\psi = y - b_\ell(x) \tag{44c}$$

$$p_u - p = - C\, b_\ell''(x)\,(\psi_u - \psi) \tag{44d}$$

$$b_u - b_\ell = \text{const.}$$

Note that Eqs. (44) are consistent with Eqs. (16). In the present small deflection context, we go beyond the analysis associated with (16) and "patch" to the outer flow to determine the slip line deflection functions $b_u, b_\ell(x)$ and the gauge functions α_0 and κ_0. The term "patch" is used in contrast to "match" in the sense that conditions are satisfied at a fixed boundary at a finite distance in the former (i.e., the slip line) in contrast to the latter where they are satisfied in an asymptotic manner, generally, at an infinite distance.

Patching is achieved using a "blending layer" at a vertical distance of $O(\delta)$ from the slip line and airfoil. The latter will not enter into the present discussion but will be considered in connection with the trailing edge behavior. The blending layer will also be used to validate the usual Taylor's series transfer of boundary conditions employed to define the outer flow. A treatment of similar blending layers is discussed in Cole[7] in connection with incompressible flows around unblown bodies of revolution. However, some different features arise in the present context. In accord with the previous remarks, we consider the shaded region shown in Fig. 7. We consider the entire external flow field R_e in Fig. 1 and in particular the blending layer as irrotational. In anticipation with matching with the outer flow, we assume that the blending layer is a perturbation on the freestream. Accordingly, the asymptotic expansions for the potential Φ and pressure are

$$\frac{\Phi}{U} = x + \mu(\delta)\varphi(x,y^*) + \cdots \ , \ x, y^* \text{ fixed}$$

where

$$y^* = y/\nu(\delta) .$$

Introducing the condition that the slip line is a streamline of the external flow, gives on the upper line $J_u = 0$ the relation

$$(1 + u\varphi_x \ , \ \frac{u}{v}\,\varphi_{y^*}) \cdot (-\delta b_u' \ , \ 1) = 0$$

$$\varphi_{y^*}\left(x \ , \ \frac{\delta}{v}\, b_u(x)\right) = \frac{v\delta}{u}\, b_u'(x) . \tag{45}$$

To preserve the structure of the second argument of the right hand side of (45), we assert that

$$\delta = v .$$

Furthermore, we obtain the most general boundary condition in (45) if we let

$$\mu = \delta^2 .$$

Now if $\Delta = \partial^2/\partial x^2 + \partial^2/\partial y^2$, we have that

$$\Delta\Phi = 0$$

which implies that one-dimensional flow given by

$$\varphi_{y^*y^*} = 0 \tag{46}$$

or

$$\varphi = a(x)y^* + b$$

$$= b_u'(x)y^* + b(x) \ , \ (b_u' = b_\ell')$$

by (45). A similar result for the lower blending layer is

$$\varphi = b_\ell' y^* + b(x) .$$

Now the well known outer expansion for the region outside the "inner" blending layer is

$$\frac{\Phi}{U} = x + \delta\phi(x,y) + \cdots$$

x, y fixed as $\delta \to 0$.

Matching of the inner and outer expansions can be achieved by introduction of an intermediate variable

$$y_\eta = \frac{y}{\eta(\delta)}$$

where $\delta << \eta << 1$. The matching condition is

$$\lim_\eta \equiv \lim_{\delta \to 0} \left[\Phi_{\text{outer}}(x,y_\eta) - \Phi_{\text{inner}}(x,y_\eta)\right] \tag{47}$$

where

$$\frac{\Phi_{\text{outer}}}{U} = x + \delta\phi(x,\eta y_\eta) + \cdots$$

$$= x + \delta\left[\phi(x,0+) + \eta y_\eta \phi_y(x,0+) + \cdots\right] + o(\delta^2) \tag{48a}$$

$$\frac{\Phi_{\text{inner}}}{U} = x + \delta\phi(x,0+) + \delta^2\left[b_u'(x)\,\frac{\eta y_\eta}{\delta} + b(x)\right] + \cdots \tag{48b}$$

where the second term of (48b) has been interposed for matching and can be construed as an additional element lumped into $b(x)$ of the dominant inner problem associated with (46). Application of (47) and a similar argument for the lower blending layer gives for matching that

$$\phi_y(x,0+) = b_u'(x) = \phi_y(x,0-) = b_\ell'(x) \tag{49}$$

which is the condition anticipated from tangent flow. Determination of $b(x)$ in (48b) depends on

the inner limit of the outer representation of the flow field as a line vortex extending to downstream infinity whose local strength is proportional to the jump in pressure across the jet $[\phi_x] \equiv \phi_x(x,0+) - \phi_x(x,0-)$. The subsequent argument should be similar in some respects to that associated with the finite line source discussed in Ref. 7. In this connection, the details of the determination of b(x) will be discussed elsewhere.

To determine the gauge functions κ_0 and α_0 appearing in (37), the static pressures of the jet are equilibrated to those of the blending layer at the slip line. From the interposed term in (48b) and Bernoulli's relation in the blending layer, the external pressure P_e is given by

$$\frac{P_e - P_\infty}{\rho U^2} = \delta p_e + \cdots \tag{50}$$

in both inner and outer limits, where on the slip lines

$$p_e(x,b_u(x)) = -\phi_x(x,0+) \tag{51a}$$

$$p_e(x,b_\ell(x)) = -\phi_x(x,0-) \ . \tag{51b}$$

From (51) and continuity of pressure across the slip line it is obvious therefore that

$$\kappa_0 = \delta \tag{52a}$$

and

$$\alpha_0 = \delta^{-1/2} \ , \ \beta_0 = \delta^{1/2} \ . \tag{52b}$$

Furthermore, Bernoulli also implies that

$$\alpha_1 = \delta^{3/2}$$

again in agreement with Eqs. (16) for the jet centerline of radius of curvature $O(\delta^{-1})$. Note that the vorticity $u_y - v_x$ of the general solution (43) is $O(\delta^{-1/2})$, although in the special case (44) it is $O(\delta^{1/2})$. This fact appears not to affect the result (44d) which is in agreement with the Spence relation obtained under the assumption of irrotational potential vortex flow for a jet element.

It is significant to note that a nonuniformity occurs near the trailing edge point C in Fig. 1. The order of the pressure perturbations in (51b) are incorrect near the trailing edge stagnation region of the flow below the slip line, i.e.,

$$\frac{P_e - P_\infty}{\rho_\infty U^2} = O(1) \ .$$

Since pressure is to be matched across the slip line, this implies a corresponding change of orders in the jet and hence, (52a) becomes invalid. This feature as well as the blending layer structure are anticipated as important aspects of the transonic problem, and are under investigation. As indicated previously, local expansions are required to deal with the nonuniformities.

External Flow

For distances large compared to the jet width, the fine structure of the jet is important only insofar as it provides matching conditions to the irrotational flow field outside itself. In incompressible flow, this external "outer" flow can be determined by thin airfoil theory. At transonic speeds, small disturbance theory is appropriate for this region. Details of the asymptotic matching procedure have been discussed for incompressible flow in the previous section. Based on these developments and the earlier ones for arbitrary deflection thin jets in Section 2.2, the boundary conditions for the outer flow in the incompressible and transonic cases for the jet flap and upper surface blowing are now indicated.

Jet Flap

Referring to Fig. 8, the equation of an airfoil can be given as

$$y = \delta f(x)$$

and the jet is

$$y = \delta g(x)$$

where δ is the thickness ratio of the airfoil, f is the upper or lower surface and involves the angle of attack which is of the same order of δ. Considering a small disturbance approximation, we obtain

$$R^{-1} = \frac{\dfrac{d^2y}{dx^2}}{\left[1 + \left(\dfrac{dy}{dx}\right)^2\right]^{3/2}} = \frac{\delta g''}{\left[1 + \delta^2 g'^2\right]^{3/2}} \doteq \delta g''(x) \ .$$

Letting the "outer" expansion pressure coefficient be represented as

$$\frac{p - p_\infty}{\rho U_\infty^2} = \delta P(x,y) + \cdots$$

then by virtue of a generalization of (42)

$$[P(x,0)] = -C_j g''(x) = -2[\phi_x] \tag{53}$$

where

$$C_j \equiv \left(\rho \int_{-\tau}^{\tau} q_\xi^2 d\eta\right) \Big/ \rho U_\infty^2 = O(1) \tag{54a}$$

and ϕ is a perturbation potential. Note that (53) can also be obtained from (44d).

Equation (53) is the relation used in conjunction with the jet tangency relation

$$\phi_y(x,0) = g'(x) \tag{54b}$$

and the airfoil boundary conditions to determine the external flow field. These relations coincide with those derived by Spence. They can be generalized for transonic flow by placing the ρ inside the integrand in (54a).

Upper Surface Blowing

To treat conditions on the blown part of the airfoil Eq. (53) can be applied by approximating the radius R by $(f'')^{-1}$ to obtain the wall pressures, and using the airfoil and jet boundary conditions to determine the upper slip line jet pressures.

From the arbitrary deflection thin jet theory derived in Section 2.2, it can be seen that rotational flow produces the same pressure jumps across the jet in the dominant approximation as the irrotational Spence models. Correspondingly, it can be shown that to within factors involving the density, qualitatively similar results are obtained for transonic flow. Another important aspect of the asymptotic representations derived here is that they lead to higher approximations for the structure of the jet and external flow which can be systematically obtained. Finally, the analytical solutions described above allow the systematic assessment of the effects of initial vorticity and skewness which are inaccessible to other theories.

3.0 Results and Discussion for Transonic Upper Surface Blowing

A successive line overrelaxation (SLOR) scheme within a Karman Guderley framework has been used to compute the flow field over an upper surface blown airfoil. On the blown portion, the jump conditions across the jet are determined by the asymptotic results given in previous sections, i.e., Eqs. (53) and (54b). Providing that the region is not too close to the jet exit or trailing edge, the streamwise gradients can be neglected in the entropy and velocity component parallel to the wall. Away from these regions, the pressure gradient perpendicular to the streamlines is balanced by centrifugal force. For the region near the jet exit, these assumptions become invalid. Here, the scale of the gradients in the streamwise direction become important, principally due to the influence of wave interactions with the slip line. Similar fine structures occur near the trailing edge where the flow can stagnate on the unblown side, depending on the ratio of the stagnation pressure of the jet to the ambient stagnation value. For incompressible flow, the previous sections have discussed the tri-stable equilibrium at the trailing edge corresponding to the value of the stagnation pressure ratio, which leads to the dividing streamline leaving tangent to the upper surface if this is greater than unity ("EL" configuration). Consistent with the previous discussion, the appropriate generalization to transonic flow was assumed also to be EL for a single valued pressure without a shock in that location. This assumption has been altered to assess the sensitivity of the flow to the dividing streamline angle. In this connection, surface pressures for the dividing streamline bisecting the trailing edge angle (as it would in incompressible flow) were compared with those for the EL arrangement. Based on these studies, significant differences are anticipated only for large incidences and trailing edge angles.

Typical results obtained from the computational model are shown in Fig. 9 in which the flow over a thick airfoil designed at Rockwell's Columbus Aircraft Division (CAD) was analyzed with the SLOR code. Here, the pressures for various values of the blowing coefficient C_j are compared against those for the unblown case at a freestream Mach number $M_\infty = 0.703$, and angle of attack $\alpha = 0°$. Substantial lift augmentation is evident for blowing. Also evident is the associated rearward motion of the shock with increased blowing and sectional loading as if the incidence is increased.

Further parametric studies are provided in Fig. 10 which indicate the effect of parallel displacement of the slot x_j (in units of the chord), on the chordwise pressures. Three positions of the slot $x_j = 0.5$, 0.65 and 0.8 are shown. No systematic trend in the blown pressures is exhibited on this airfoil with downstream slot movement for fixed C_j. Evident however is a slight intensification of the terminating shock with slot downstream motion although its position remains unaltered. Despite the limitations of the model to describe the fine structure of the jet exit region, a small suction peak which has been observed in experiments is exhibited in this vicinity for $x_j = 0.5$. In Fig. 11, the corresponding increase in lift coefficient C_L with slot downstream movement is also shown as well as the increase in the size of the supersonic region.

In Fig. 12, the increase of lift with blowing coefficient as well as size of the supersonic region is quantified.

Tests of the adequacy of the foregoing model to simulate realistic transonic USB airfoil flows have been inhibited by the lack of suitable experimental data. Information exists only for highly three-dimensional configurations, large thickness, or incidence in ranges beyond the validity of the assumptions of small disturbance theory. Another restriction is the unavailability of the associated geometric data and flow diagnostics accompanying the tests. The results of Yoshihara and his coworkers were useful in this connection and allowed us to compare the jet flap specialized version of the USB theory in Ref. 2. For the simulations described in this paper, tests performed by N.C. Freeman at NPL on a USB modified 6% thick RAE 102 airfoil and described in Ref. 9, appear to be the most suitable results for comparison at present. Unfortunately, the angle of attack associated with the NPL data is 6° which is marginal for the application of a small disturbance model.

Figure 13 indicates comparisons of chordwise pressures for various values of C_j. Also shown are schlierens indicating the associated flow field structure. Turning to the $C_j=0$ results (Part (a)), massive shock induced separation is indicated and is apparently initiated at the downstream limb of the lambda shock on the upper surface. This is reflected in the classical erosion of the suction plateau and is responsible for the indicated disagreement between the inviscid computational results and the data. For these tests, nominal tangential blowing with a slot height of 0.07% of the chord was used. The slot location is 15% downstream of the nose. The Mach number M immediately above the slip line at the slot (point A in Fig. 1) is approximately 1.29 for both C_j's indicated. For $C_j=0.017$, the slot Mach number M_e has been estimated as 1.79 and for $C_j = 0.048$, $M_e \approx 2.36$.

Comparison between theory and experiment in Part (b) of Fig. 13 indicates reduced discrepancies on the upper surface associated with the limited separation. In Part (c), the agreement is correspondingly further improved.

To achieve adequate realism, it is important to discuss factors responsible for the disagreements. One feature not captured by the USB simulation is the pressure spike at the slot location. Based on the slot size, the streamwise scale for this phenomenon is at least an order of magnitude greater than the characteristic wavelength of a Mach diamond pattern in the wall jet. These fluctuations may not be resolvable with conventional pressure tap arrangements for the thin slot employed in the tests. If a rough model of a coflowing inviscid supersonic wall jet over a flat plate is used to describe the flow near the slot, the approach to a final steady state may be damped oscillatory or monotone depending on whether the reflection coefficient R which is given by

$$R = \frac{\lambda - 1}{\lambda + 1} \tag{55}$$

where

$$\lambda = M_e^2 \beta / M^2 \beta_e \ , \ \beta = \sqrt{M^2 - 1} \ , \ \beta_e = \sqrt{M_e^2 - 1}$$

is respectively positive or negative.

The relaxation length L to achieve the downstream pressure in units of the exit height is of the order of $\ln R$ which can be approximately 5 to 50 in the present case depending on the accuracy of the estimate for M_e. Note in this connection that

$$R < 0 \quad \text{for} \quad 1 \leq M \leq \frac{M_e^2}{\beta_e} \ , \text{ and } M_e \leq M \leq \infty$$

$$R \geq 0 \quad \text{for} \quad \frac{M_e^2}{\beta_e} \leq M \leq M_e \ .$$

For the submerged case, $R \to 1$, $(M_e >> M)$, and the Prandtl periodic pattern is obtained, with no radiation of energy to the external flow.

These facts suggest that one factor that may be responsible for the observed spike is the internal decay process in the jet. If transonic effects and wall curvature are accounted for, the presence of "ballooning" and throats in the jet may also be contributory. We have discussed such phenomena in connection with submerged transonic wall jets in Ref. 10 and have reported analogous results for the coflowing case in Ref. 11. Selection rules in terms of M_e and M for the existence of throats in the jet near field are given in Ref. 12 which are based on an integral form of the Karman Guderley equation. A rough sketch of the wave system that could explain the spikes in Figs. 13b and 13c is shown in Fig. 14. Yet another phenomenon that would have a similar wave pattern would be a slight upward motion of the jet due to viscous mixing or a misalignment with the surface tangent at point A.

Turning now to the discrepancy of the values shown on the rear surface (downstream of 0.5c) in Fig. 13c, we note that in spite of the obvious elimination of separation, a thick viscous wall jet is present. Downstream diffusion will affect the application of the Spence relation on the blown portion as well as the shock jump. In view of the wall jet thickness shown on the schlierens, this factor appears to be more significant than shock obliqueness at its foot. A near term refinement is being implemented employing a coupled inviscid-viscous model using second order boundary layer corrections to the Spence boundary conditions accounting for axial gradients of the displacement and momentum thickness. Once these refinements are incorporated, systematic optimization between separation suppression, wave drag minimization, and supercirculation control will be possible. It is envisioned that the design techniques contained in Refs. 13-15 will augment this capability by providing methods to modulate shock formation in concert with the blowing effects.

4.0 Conclusions

Asymptotic and computational models have been used to obtain the flow over upper surface blown (USB) airfoils in incompressible and transonic flow. The treatment involves a detailed analysis of the flow in the jet. The analytical and computational results indicate that

- In the thin jet small deflection approximation, the pressure jumps associated with the Spence theory prevail even if the flow is rotational and compressible.
- The asymptotic developments provided allow further systematic refinements.
- Effects associated with initial skewness and vorticity inaccessible to other theories can be assessed.
- The dividing streamline leaves tangent to the upper surface in incompressible flow.
- Computational results obtained for transonic USB configurations indicate significant enhancements of lifting pressures associated with blowing.
- Comparisons with experiment indicate the need for refinements incorporating wave interaction phenomena near the jet exit as well as viscous interaction processes in the downstream portion of the wall jet.

References

1. Spence, D.A., "The Lift Coefficient of a Thin Jet Flapped Wing," Proc. Roy. Soc., Ser. A., 238, December 1956, pp. 46-48.
2. Malmuth, N.D. and Murphy, W.D., "A Relaxation Solution for Transonic Flow over Jet Flapped Airfoils," AIAA J., 14, September 1976, pp. 1250-1257.
3. Murphy, W.D. and Malmuth, N.D., "A Relaxation Solution for Transonic Flow over Three-Dimensional Jet-Flapped Wings," AIAA J., 15, January 1977, pp. 46-53.
4. Murman, E.M. and Cole, J.D., "Calculation of Plane Steady Transonic Flows," AIAA J., 9, January 1971, pp. 114-121.

5. Malmuth, N.D. and Murphy, W.D., "An Inviscid Model for Submerged Transonic Wall Jets," AIAA Paper 77-174 (1977).
6. Melnik, R.E., Chow, R., and Mead, H.R., "Theory of Viscous Transonic Flow Over Airfoils at High Reynolds Number," AIAA Paper 77-680 (1977).
7. Cole, J.D., Perturbation Methods in Applied Mathematics, Ginn and Blaisdell, Waltham, Mass. (1968).
8. Yoshihara, H., Carter, W.V., Fatta, J.G. and Magnus, R.G., "Aeronautical Exploratory Research on Jet Flapped Airfoils," Convair Report L-112173, February 1972.
9. Pearcey, H.H., "Shock Induced Separation and Its Prevention by Design and Boundary Layer Control," Boundary Layer and Flow Control, Lachmann, G.V., ed., Pergamon, Oxford, London, 1961, pp. 1166-1344.
10. Malmuth, N. and Murphy, W.D., "An Inviscid Model for Submerged Transonic Wall Jets," AIAA Paper 77-174 (1977).
11. Malmuth, N. and Murphy, W.D., Quarterly Letter Progress Report No. 14 on ONR Contract N00014-76-C-0350, SC5055.14QR, August 20, 1979.
12. Malmuth, N. and Murphy, W.D., Quarterly Letter Progress Report No. 13 on ONR Contract N00014-76-C-0350, SC5055.13QR, May 14, 1979.
13. Shankar, V., Malmuth, N.D. and Cole, J.D., "Computational Transonic Airfoil Design in Free Air and A Wind Tunnel," AIAA Paper 78-103, AIAA 16th Aerospace Sciences Meeting, Huntsville, Alabama, January 16-18, 1978.
14. Shankar, V., Malmuth, N.D. and Cole, J.D., "A Consistent Design Procedure for Supercritical Airfoils in Free Air and A Wind Tunnel," invited paper presented at NASA Langley Conference on Advanced Technology Research, also in Proceedings, March 1978.
15. Shankar, V., Malmuth, N.D. and Cole, J.D., "A Computational Inverse Procedure for Three-Dimensional Wings and Wing-Body Combinations," AIAA Paper 79-0344, presented at the 17th Aerospace Sciences Meeting, New Orleans, Louisiana, January 15-17, 1979.

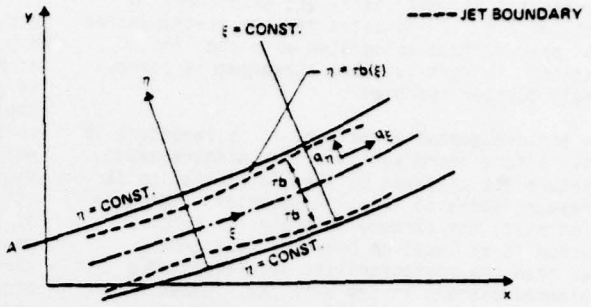

Fig. 2. Section of Jet and Curvilinear Coordinate System

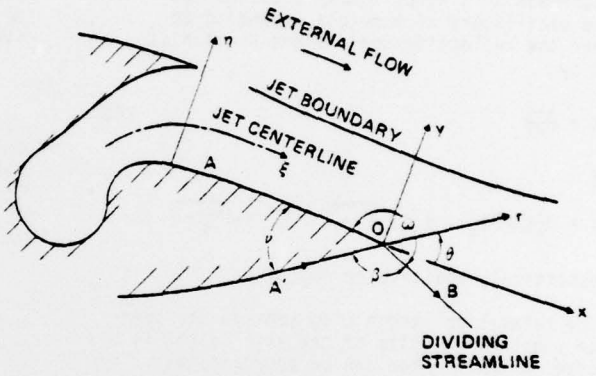

Fig. 3. Blown Trailing Edge Formulation

$$L[\Phi] = (a^2 - \Phi_x^2)\,\Phi_{xx} - 2\,\Phi_x\Phi_y\Phi_{xy} + (a^2 - \Phi_y^2)\,\Phi_{yy} = 0$$

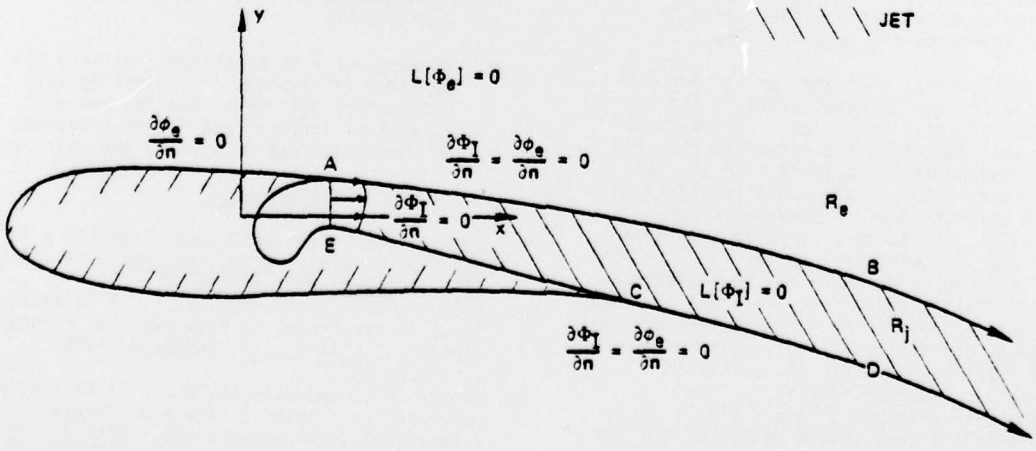

Fig. 1. Transonic Upper Surface Blowing – Full Potential Equation Formulation

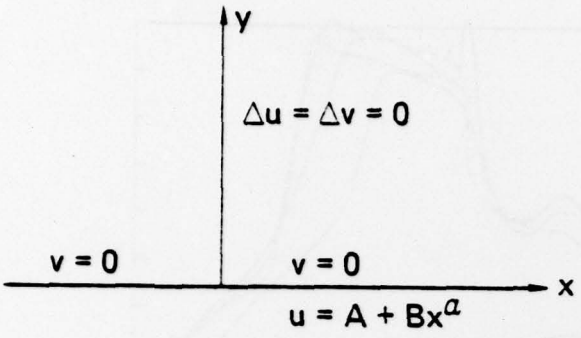

Fig. 4. Jet Trailing Edge Boundary Value Problem

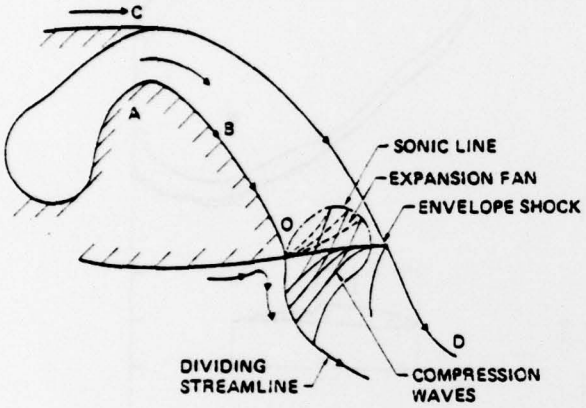

Fig. 5a. Multivalued Pressure at Trailing Edge – Configuration for Dividing Streamline (Discontinuous Configuration)

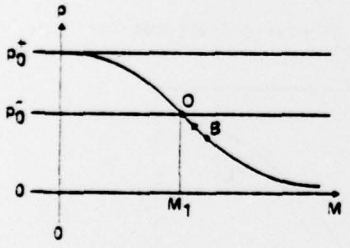

Fig. 5b. Continuous Isentropic Recompression

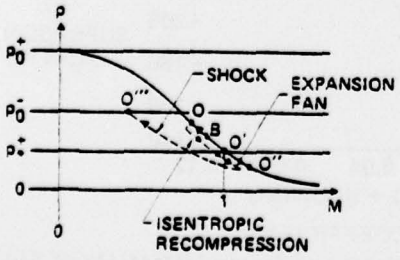

Fig. 5c. Discontinuous Configuration

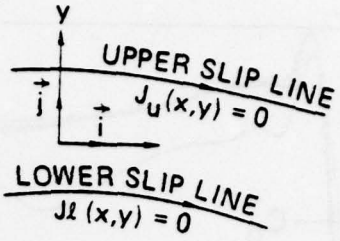

Fig. 6. Jet Flow Geometry

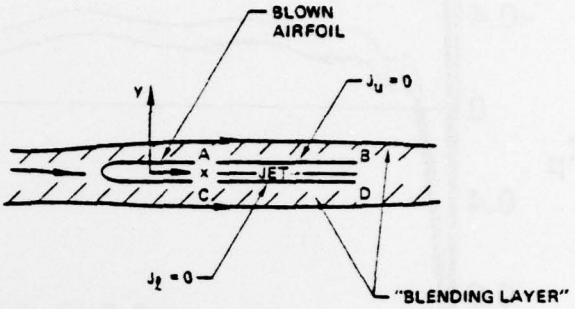

Fig. 7. Blending Layer Schematic

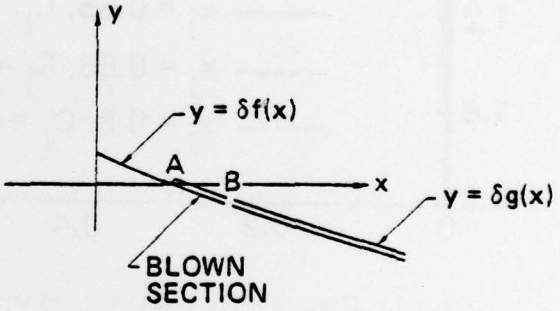

Fig. 8. Configuration for Outer USB Problem

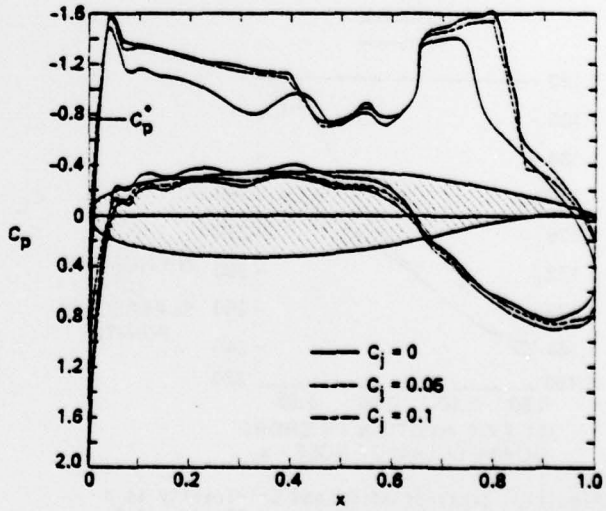

Fig. 9. Effect of Blowing Coefficient, (C_j), Variations on Chordwise Pressures for CAD USB Supercritical Airfoil, M_∞=0.703, α=0°, (Slot Location at 65% Chord).

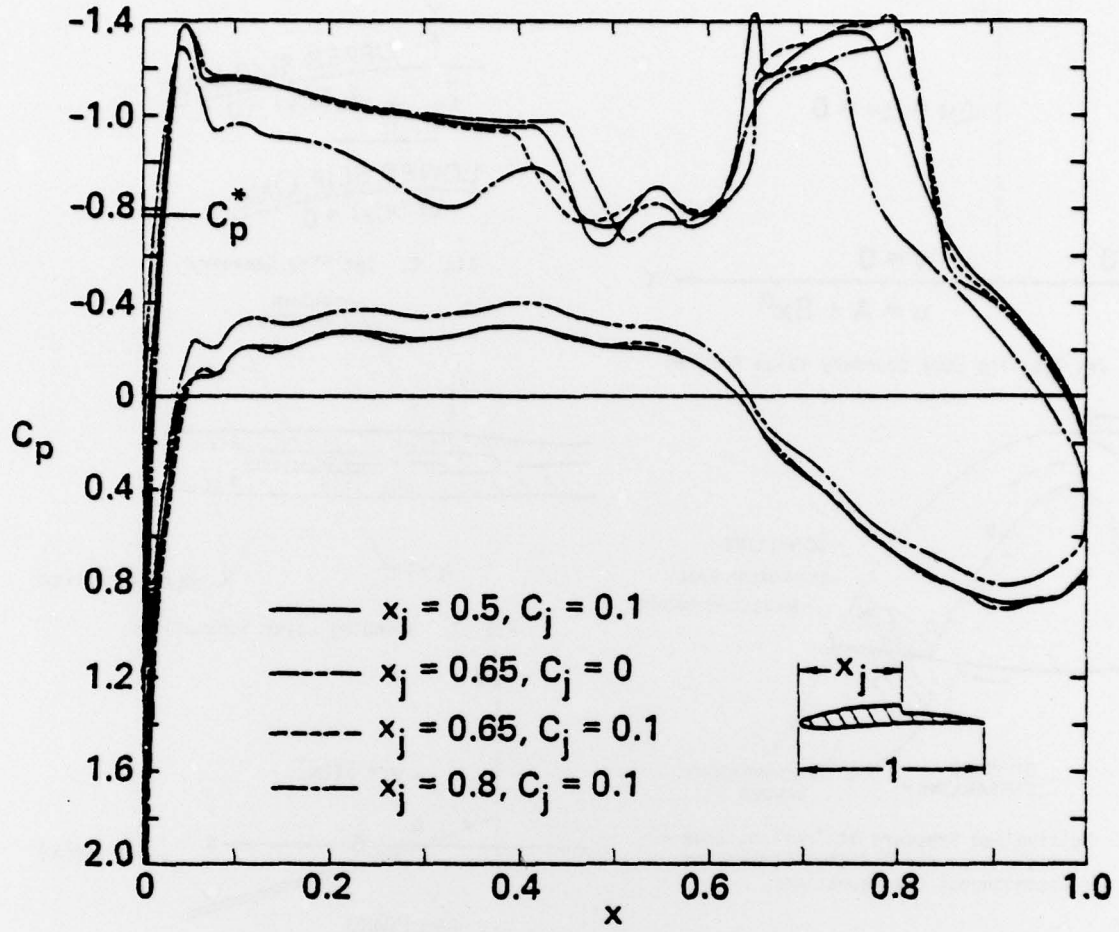

Fig. 10. Effect of Slot Location x_j in Units of Chord on Chordwise Pressures for CAD USB Supercritical Airfoil, $M_\infty = 0.703$, $\alpha = 0°$.

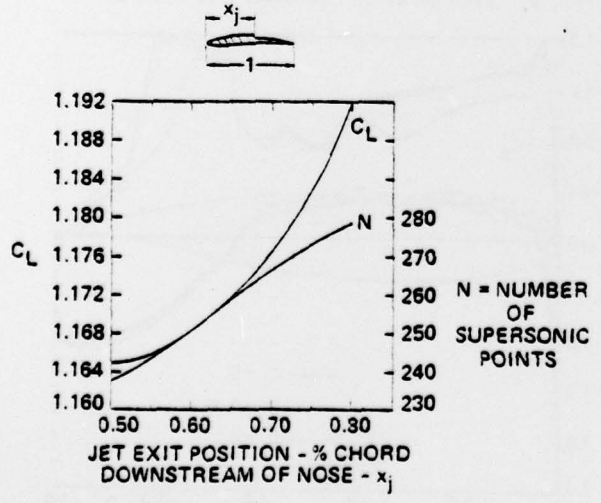

Fig. 11. Behavior of C_L and Criticality as a Function of Extent of Blowing, CAD USB Airfoil, C_j=0.1, M_∞=0.703, α=0°.

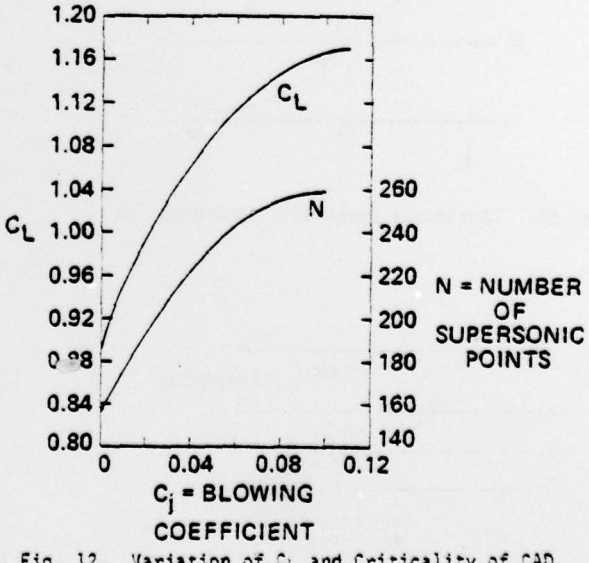

Fig. 12. Variation of C_L and Criticality of CAD USB Airfoil with Blowing Coefficient, $M_\infty = 0.703$, $\alpha = 0°$, $x_j = 0.65$.

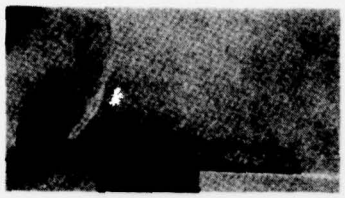

(a) $C_j = 0$

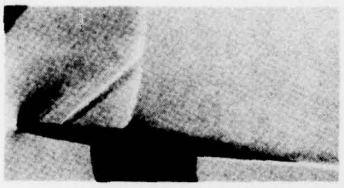

(b) $C_j = 0.017$

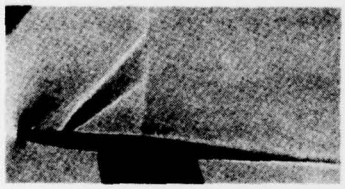

(c) $C_j = 0.048$

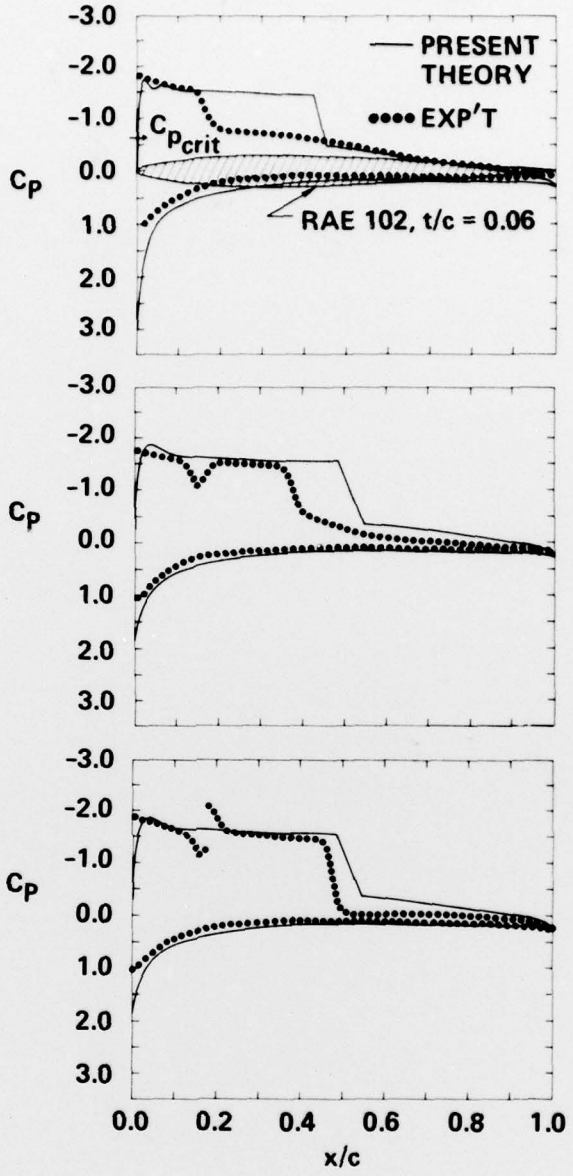

Fig. 13. Comparison of USB Theory of This Paper with NPL Tests of Freeman (Ref. 9), M_∞=0.75, α=6°, c=Chord, t=Maximum Thickness

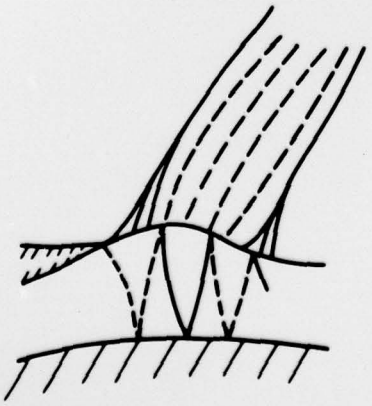

Fig. 14. Inviscid Wave Pattern Associated with Slip Line Ballooning and Jet Throat Formation